

## Research Article

# Effect of Ca Concentration on Microstructure and Mechanical Properties of As-Cast and As-Extruded Quasicrystal-Strengthened Mg-7.2Zn-2.4Gd Alloy

Jianchun Sun,<sup>1</sup> Yilong Ma,<sup>1</sup> Hongwei Miao ,<sup>2</sup> Kejian Li ,<sup>1</sup> Chunhong Li,<sup>1</sup> and Hua Huang <sup>2</sup>

<sup>1</sup>School of Metallurgy and Materials Engineering, Chongqing University of Science and Technology, Chongqing 401331, China

<sup>2</sup>National Engineering Research Center of Light Alloy Net Forming and State Key Laboratory of Metal Matrix Composite, Shanghai Jiao Tong University, Shanghai 200240, China

Correspondence should be addressed to Hongwei Miao; miaohongwei@sjtu.edu.cn and Hua Huang; huangh@sjtu.edu.cn

Received 9 July 2018; Accepted 17 September 2018; Published 15 October 2018

Academic Editor: Pavel Lejcek

Copyright © 2018 Jianchun Sun et al. This is an open access article distributed under the Creative Commons Attribution License, which permits unrestricted use, distribution, and reproduction in any medium, provided the original work is properly cited.

Quasicrystal-strengthened Mg-Zn-RE (RE = rare-earth element) alloys have been investigated extensively due to their excellent mechanical properties. Here, we prepare quasicrystal-strengthened Mg-7.2Zn-2.4Gd (wt.%) alloy with different concentrations of Ca addition (0, 0.16, 0.32, and 0.64 wt.%) by traditional gravity casting, followed by extrusion at 573 K with the extrusion ratio of 9 : 1. The microstructure and room temperature tensile properties of as-cast and as-extruded alloys are characterized. With the addition of the trace amount of Ca, the I-phase tends to transfer into W-phase due to the appearance of Mg<sub>2</sub>Ca and Mg<sub>6</sub>Zn<sub>3</sub>Ca<sub>2</sub>. As a consequence, the mechanical properties of the as-cast Ca containing alloys are downgraded. After extrusion, in comparison to the as-cast alloys, microstructure of the four types of alloys is refined and mechanical property is enhanced greatly. With the increasing of Ca concentration, the grain size is decreased gradually. However, the yield strength of the alloys is decreased to about 230 MPa and then up to 269 MPa, while the elongation increases first from 12.9% to 13.6% yet then decreases to 9.9%.

## 1. Introduction

After the first discovery of a quasicrystalline phase by Shechtman et al. in 1984 [1], a lot of studies have been carried out on the structure and properties of the quasicrystal phase. Researchers originally thought that the quasicrystal phase only can be formed during high cooling rate solidification. Until Luo et al. [2] found quasicrystals can be formed in traditional casting Mg-Zn-RE alloys, the magnesium alloys reinforced with quasicrystals, such as Mg-Zn-Y [3–6] and Mg-Zn-Gd [7–12] alloys, are receiving considerable attention and eliciting widespread interest in materials world. I-phase has many advantages such as high hardness, high thermal stability, low coefficient of friction, and low interfacial energy [13], and it was reported that there was a definite orientation relationship and good atomic match between I-phase and  $\alpha$ -Mg matrix, which leads to the high tensile strength of 308 MPa and the large plasticity of

16.4% of Mg-Zn-Gd alloy at room temperature [10, 14]. In addition, the Mg-Zn-Gd alloy also shows a high strength of 117 MPa and a high elongation of 82.5% at 473 K due to the high thermal stability of I-phase and the high cohesion of I-phase with the matrix [15]. Therefore, the Mg-Zn-RE alloy reinforced with I-phase shows a good prospect of application.

Lots of works have been done on Mg alloys containing Ca [16–18] and found that Ca addition can refine the grain size and improve the high-temperature behavior of magnesium alloys [19]. For example, the grain size of the as-cast Mg-Zn-Mn-Ca significantly decreased with the increasing of Ca content up to 0.5 wt.% [16], and Chen et al. [20] reported that the microstructure of the AZ91 magnesium alloy is clearly refined with Ca addition. After thermal-mechanical processing, Ca can strengthen and toughen the Mg alloys by the newly formed Ca-containing particles, which can retard the growth of the dynamic recrystallization grains and refine

the grain size of extruded Mg-Zn-Ca alloys [18]. In addition, Zhang et al. [17] reported that with a low content of Ca from 0 to 0.5%, the extrusion textures were greatly weakened due to the particle stimulated nucleation of recrystallization (PSN), and then tensile properties of the alloys increased obviously. However, the addition of the Ca for magnesium is limited, further increasing of Ca content higher than 0.5 wt.% for as-cast Mg-Zn-Mn-Ca did not refine the grain more [16], and the mechanical properties decreased after 2 wt.% addition of Ca for AZ91 magnesium alloy due to the  $Al_4Ca$  phases distributed at the grain boundaries [20]. Therefore, adding trace amount of Ca is beneficial to grain refinement, texture randomization, and tensile mechanical properties improvement, and excessive addition of Ca is harmful to mechanical properties.

Aiming to improve the mechanical properties of the Mg-Zn-Gd alloys reinforced with I-phase, Ca was selected for alloying element in this study. Different Ca concentrations were selected for addition into Mg-7.2Zn-2.4Gd alloy. The microstructure and mechanical properties of as-cast and as-extruded Mg-7.2Zn-2.4Gd- $x$ Ca ( $x=0, 0.16, 0.32, \text{ and } 0.64 \text{ wt.}\%$ ) alloys were characterized, and the effects of the Ca addition on quasicrystal-strengthened Mg-7.2Zn-2.4Gd alloy were discussed.

## 2. Experimental Procedures

Four studied alloys with a nominal composition of Mg-7.2Zn-2.4Gd- $x$ Ca ( $x=0, 0.16, 0.32, \text{ and } 0.64 \text{ wt.}\%$ ) were designed for this study. These alloys were prepared by using electric resistance melting and traditional gravity casting with pure Mg (99.9%), Zn (99.9%), Mg-87%Gd (wt.%), and Mg-30%Ca (wt.%) master alloys under the protection of a mixed gas atmosphere containing  $SF_6$  (1 vol.%) and  $CO_2$  (99 vol.%). The melt was homogenized at 1023 K for half an hour and then cooled to 1003 K. Then the melt was poured into a steel mould which was preheated to 473 K. The ingots used for extrusion were machined into billets with a dimension of 60 mm in diameter and 60 mm in height. These billets were preheated at 573 K for 1 hour before extrusion and then extruded at 573 K with an extrusion ratio of 9:1 at a speed of  $2 \text{ mm} \times \text{s}^{-1}$  followed by cooling in water.

For optical microscopy (OM) observations, the as-cast samples were etched by 4% nitric acid + 96% alcohol, and the as-extruded samples were etched with an etchant containing 1 g of oxalic acid + 1 ml of nitric acid + 1 ml of acetic acid + 150 ml of distilled water. To characterize the composition of the second phase, energy dispersive X-ray spectroscopy (EDS) analysis and X-ray diffraction (XRD) with the  $Cu K\alpha$  radiation were conducted. Tensile tests were performed at room temperature on a Zwick/Roell Z020 testing machine. The extruded rods were cut into dog bone tensile test specimens (specimen gauge of 15 mm in length) along the extrusion direction and then grinded by SiC papers. At least three specimens were tested with an initial strain rate of  $0.6 \text{ mm} \times \text{s}^{-1}$  for each alloy.

## 3. Results

**3.1. Microstructure and Mechanical Properties of As-Cast Alloys.** The optical microstructures of as-cast Mg-Zn-Gd

(-Ca) alloys are shown in Figure 1. The Ca-free alloy exhibits a dendritic microstructure (Figure 1(a)), which was mostly composed of I-phase,  $Mg_4Zn_7$ , and a little W-phase as reported in our previous study [10, 12]. With the addition of Ca from 0.16 wt.% to 0.32 wt.%, when the Ca addition increased to 0.64%, the amount of the second phase was larger than the other three alloys, and most of the second phase tends to become mesh like (Figure 1(d)).

In order to further identify the composition of the second phase and find out the phase evolution after the different addition of Ca, X-ray diffraction analysis (XRD) was conducted and the results are shown in Figure 2, which reveals that the second phase in Ca-free alloy mostly consists of  $Mg_4Zn_7$  and I-phase as mentioned above. With the addition of Ca, there appears  $Mg_2Ca$  and  $Mg_6Zn_3Ca_2$  in the alloys, which is consistent with the previous study about Mg-Zn-Ca alloy [18, 19, 21].

In addition, it is interesting to note that the peak of I-phase tends to disappear with the increasing of Ca addition while the peak of W-phase tends to be more obvious. To confirm this second phase transition, SEM observation and EDS analysis were conducted. The SEM images of as-cast alloys are shown in Figure 3; it can be seen that the second phase is mostly dendritic-like, and the island-like second phase increased with the increase of Ca content which was consistent with the optical observation. And the EDS analysis results of the points marked in Figure 3 are listed in Table 1. It is clear to see that with the increase of the amount of Ca addition, the second phase changed from I-phase to W-phase with the appearance of Ca containing phases such as  $Mg_2Ca$  and  $Mg_6Zn_3Ca_2$ , which confirms the result of XRD. In addition, it can also be seen that the island-like phase which increased with Ca content was the Ca-containing phase as shown in Table 1.

Therefore, with the addition of Ca, there were more Ca-containing phases such as  $Mg_2Ca$  and  $Mg_6Zn_3Ca_2$  appearing in the alloys, which can cause the amount of Zn combined with Gd decreased. As a consequence, the I-phase tends to transfer to W-phase which has low Zn content. The island-like second phase which appeared after the addition of Ca was detected as the Ca-containing phase. And when the addition of Ca increased to 0.64%, the I-phase was hardly detected in the alloy and more Ca-containing phase generated, the volume fraction of the second phase increased, and the microstructure tended to be mesh like.

Figure 4 shows the representative tensile stress-strain curves of the as-cast alloys. It can be seen that the ultimate tensile strength (UTS), yield strength (YS), and elongation of as-cast Mg-7.2Zn-2.4Gd are 205 MPa, 58 MPa, and 7.1%, respectively. However, it is obvious to see that, with the addition of Ca, the UTS, YS, and elongation were all decreased. The YS increased from 49 MPa to 55 MPa with the increase in Ca addition from 0.16% to 0.64% due to the increase of the second phase. The elongation increased a little from 6.9% to 7.2% with the increase in Ca addition from 0.16% to 0.32%, while decreased to 6.5% when the Ca addition increased to 0.64% due to the stress concentration around the large second phase which can be found more in the 0.64% Ca-containing alloy, and this stress concentration can finally lead to fracture.

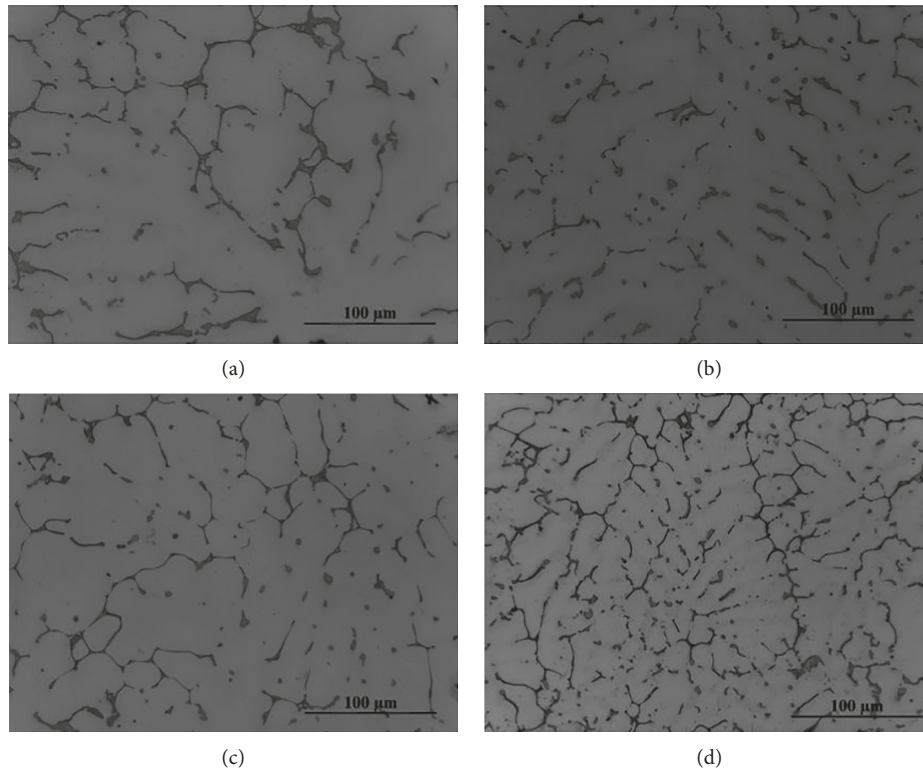


FIGURE 1: Optical micrographs of the as-cast Mg-Zn-Gd(-Ca) alloys: (a) Mg-7.2Zn-2.4Gd, (b) Mg-7.2Zn-2.4Gd-0.16Ca, (c) Mg-7.2Zn-2.4Gd-0.32Ca, and (d) Mg-7.2Zn-2.4Gd-0.64Ca.

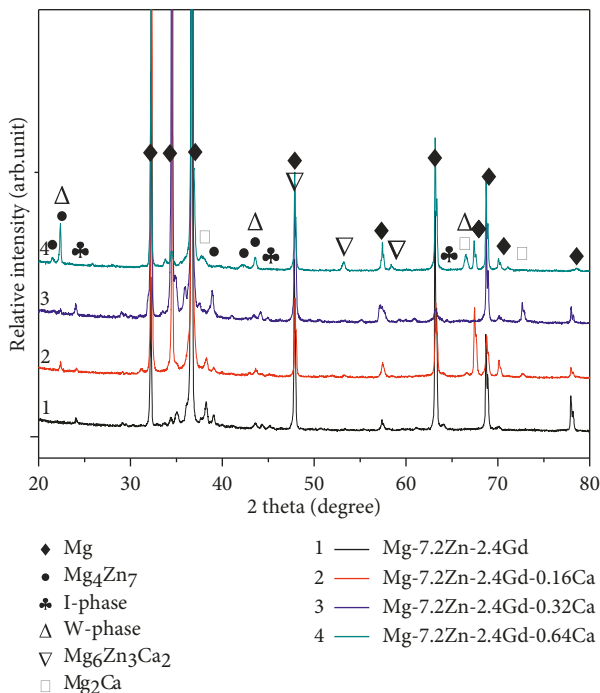


FIGURE 2: XRD result of the as-cast Mg-Zn-Gd(-Ca) alloys.

**3.2. Microstructure and Mechanical Properties of As-Extruded Alloys.** Figure 5 shows the microstructures of the as-extruded Mg-Zn-Gd(-Ca) alloys which were extruded at

573 K with an extrusion ratio of 9. The dendritic second phase was crushed and distributed along the extrusion direction as the form of black band structure which can be found in Figure 5. It can be seen that the black band structure increased with the increase in the addition of Ca.

Figure 6 shows the representative tensile stress-strain curves of the as-extruded alloys. It can be seen that the mechanical properties were greatly enhanced after being extruded. The ultimate tensile strength (UTS), yield strength (YS), and elongation of as-extruded Mg-7.2Zn-2.4Gd are 286 MPa, 250 MPa, and 12.9%, respectively. With the increase in Ca addition to 0.16% and 0.32%, the YS decreased to 230 MPa and 234 MPa, respectively, while the elongation does not have obvious improvement, which was around 13.6%. It is obvious that the elongation decreased to 9.9% when the Ca addition increased to 0.64%, while the YS improved sharply to 269 MPa.

## 4. Discussion

**4.1. Effect of Ca Addition on Microstructure.** During the solidification of Mg-Zn-Ca alloys, a binary eutectic reaction ( $L \rightarrow \alpha\text{-Mg} + \text{Mg}_2\text{Ca}$ ) occurs at about 430°C and then a second binary eutectic reaction ( $L \rightarrow \alpha\text{-Mg} + \text{Mg}_6\text{Zn}_3\text{Ca}_2$ ) occurs at about 400°C when the Zn/Ca atomic ratio is more than 1.2 [21]. In this study, the Zn/Ca atomic ratio is far more than 1.2, so  $\text{Mg}_2\text{Ca}$  and  $\text{Mg}_6\text{Zn}_3\text{Ca}_2$  might precipitated in the matrix during solidification. XRD analysis (Figure 2) confirmed that  $\text{Mg}_2\text{Ca}$  and  $\text{Mg}_6\text{Zn}_3\text{Ca}_2$  were precipitated during

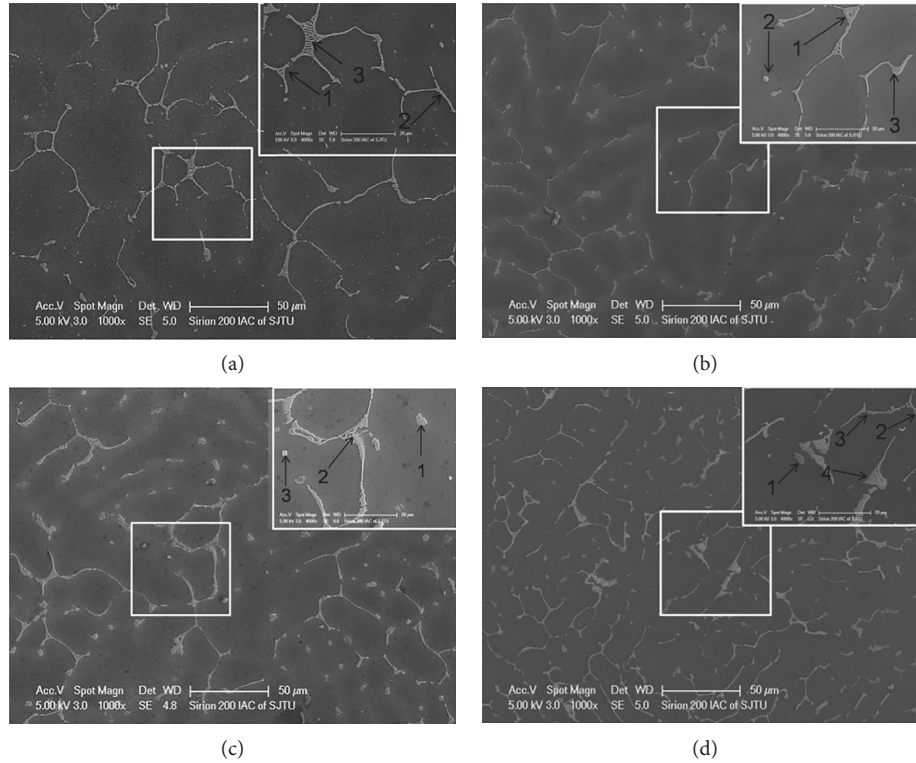


FIGURE 3: SEM images of the as-cast Mg-Zn-Gd(-Ca) alloys: (a) Mg-7.2Zn-2.4Gd, (b) Mg-7.2Zn-2.4Gd-0.16Ca, (c) Mg-7.2Zn-2.4Gd-0.32Ca, and (d) Mg-7.2Zn-2.4Gd-0.64Ca.

TABLE 1: EDS result of the as-cast alloys.

Alloys	Point	Mg	Zn	Gd	Ca	Possible phase
Mg-7.2Zn-2.4Gd	1	43.06	47.74	9.2	—	I-phase
	2	78.79	17.95	3.26	—	I-phase
	3	76.23	21.01	2.76	—	I-phase + Mg <sub>4</sub> Zn <sub>7</sub>
Mg-7.2Zn-2.4Gd-0.16Ca	1	68.5	27.38	3.85	0.27	I-phase + Mg <sub>4</sub> Zn <sub>7</sub>
	2	77.56	19.84	0.14	2.46	Mg <sub>6</sub> Zn <sub>3</sub> Ca <sub>2</sub> + Mg <sub>4</sub> Zn <sub>7</sub>
	3	60.18	33.38	6.43	0.01	I-phase
Mg-7.2Zn-2.4Gd-0.32Ca	1	94.28	4.50	0.84	0.38	I-phase
	2	92.31	5.56	2.12	0.01	W-phase
	3	98.89	0.92	0.07	0.12	Mg <sub>6</sub> Zn <sub>3</sub> Ca <sub>2</sub> + Mg <sub>4</sub> Zn <sub>7</sub>
Mg-7.2Zn-2.4Gd-0.64Ca	1	88.45	9.08	2.03	0.44	W-phase + Mg <sub>6</sub> Zn <sub>3</sub> Ca <sub>2</sub>
	2	82.85	11.58	5.44	0.12	W-phase + Ca-containing phase
	3	87.51	8.56	3.81	0.12	W-phase + Ca-containing phase
	4	77.69	15.20	6.95	0.16	W-phase + Ca-containing phase

solidification. The EDS analysis confirmed further that the island-like second phase in OM images (Figure 1) and SEM images (Figure 3) is Mg<sub>2</sub>Ca and Mg<sub>6</sub>Zn<sub>3</sub>Ca<sub>2</sub>. At the same time the precipitation of Mg<sub>2</sub>Ca and Mg<sub>6</sub>Zn<sub>3</sub>Ca<sub>2</sub> consumed the Zn element. As we know, the Zn/Gd ratio has an effect on the secondary formation of quasicrystal-strengthened Mg-Zn-Gd. Therefore, with the addition of Ca, there were more Ca-containing phases such as Mg<sub>2</sub>Ca and Mg<sub>6</sub>Zn<sub>3</sub>Ca<sub>2</sub> appearing in the alloys, which can cause the amount of Zn combined with Gd to decrease. As a consequence, the I-phase tends to transfer to W-phase which has low Zn content. The island-like second phase (Figure 3), which appeared after the addition of Ca, was detected as the Ca-containing phase. And when the addition of

Ca increased to 0.64%, the I-phase was hardly detected in the alloy and more Ca-containing phases generated, the volume fraction of the second phase increased, and the microstructure tended to be mesh like.

Ca can refine the grain size of deformed magnesium alloys [16–18]. In this study, with the Ca addition increased from 0 to 0.64%, the recrystallization during the hot extrusion was more complete, and the grain size was significantly refined. With the increase of Ca, there are more second phase precipitated in the alloys after solidification (Figure 1), which are crushed during deformation (Figure 5) and can block the dislocation during hot extrusion. Then, the accumulation of dislocation can accelerate the dynamic recrystallization,

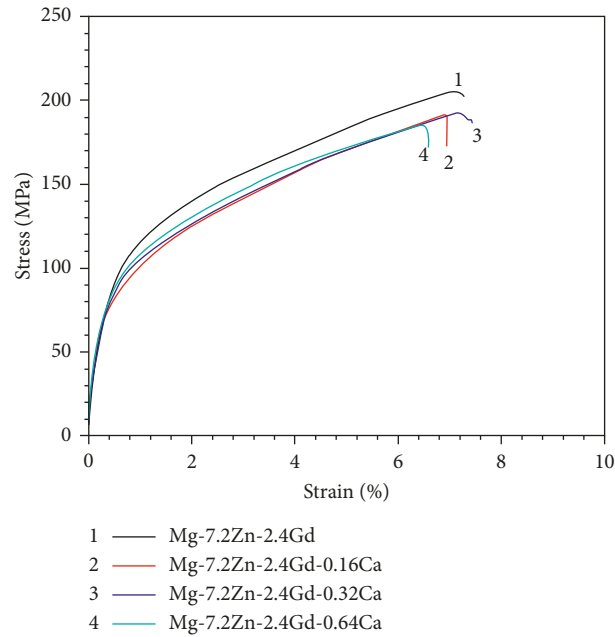


FIGURE 4: Tensile stress-strain curves of the as-cast Mg-Zn-Gd(-Ca) alloys.

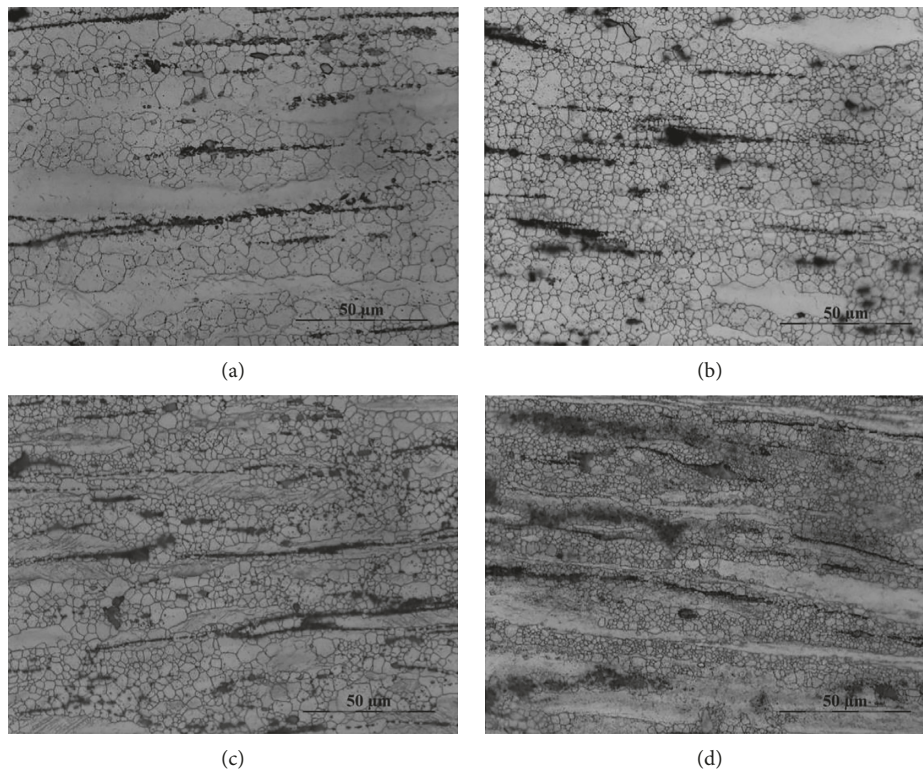


FIGURE 5: Optical micrographs of the as-extruded Mg-Zn-Gd(-Ca) alloy: (a) Mg-7.2Zn-2.4Gd, (b) Mg-7.2Zn-2.4Gd-0.16Ca, (c) Mg-7.2Zn-2.4Gd-0.32Ca, and (d) Mg-7.2Zn-2.4Gd-0.64Ca.

which is similar to the particle-stimulated nucleation (PSN) [22, 23]. On the contrary, the crushed second phase can retard the grain growth of the dynamic recrystallization at the same time. Therefore, with the Ca addition, the grain of the deformed alloys refined and volume fraction of the recrystallization grains increased (Figure 5).

**4.2. Effect of Ca Addition on Mechanical Properties.** The interface between intermetallic particles and the matrix is very important to tensile properties. When the interfacial strength is weak, cracks will easily initiate at this zone and then propagate along the interface, finally resulting in the failure of Mg alloys in the early stage during tensile tests [24].

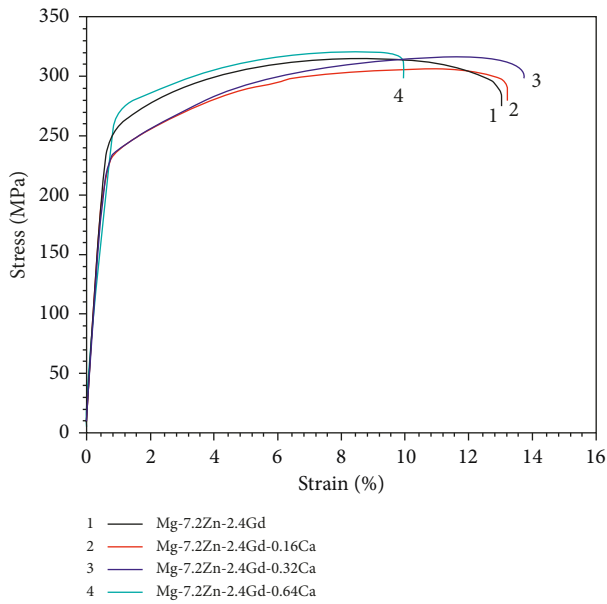


FIGURE 6: Stress-strain curves at room temperature of the as-extruded Mg-Zn-Gd(-Ca) alloys.

Hence, with the increase of the volume fraction of the secondary phase, the strength of the alloys will increase and compensate with the decrease in elongation. However, previous studies confirmed that the interface between I-phase and matrix is smooth, and the high symmetry of I-phase provides greater chances that one of its faces will have a local atomic match with one of the planes of the matrix, so the I-phase is unlikely to be a source of cracks [12, 14, 15]. Therefore, the decrease of the tensile properties of the as-cast alloys with Ca addition may be caused by the decrease of I-phase and the increasing of crystal second phase such as W-phase and Ca-containing phase, although the grain size was refined after Ca addition.

For the three as-cast Ca-containing Mg-7.2Zn-2.4Gd alloys, on one hand, grain size refined by Ca addition is beneficial to strength and elongation increment; on the other hand, I-phase precipitates transformed to W-phase and Ca-containing phases, such as  $Mg_2Ca$  and  $Mg_6Zn_3Ca_2$ , which is harmful for mechanical properties. Hence, Ca addition has a best value. The effect of Ca concentration on the mechanical properties of the as-cast alloys can be concluded according to Figure 4. With the increasing of the Ca concentration from 0.16 to 0.64 wt.%, the YS increased gradually; although the absolute increment is only 6 MPa, the increasing rate is about 12%. The UTS is basically decreased gradually, and it is rapidly worsened with the increase of Ca addition. The elongation increased in the first stage and then decreased. Therefore, the optimized concentration of Ca addition is about 0.32 wt.% for as-cast Mg-7.2Zn-2.4Gd alloy in this study.

After extrusion, the grain size was refined obviously by dynamical recrystallization and the second phase was broken into small particles, which greatly contributed to the increment of tensile properties. For the four as-extruded alloys, the effect of Ca concentration on the tensile properties

of the alloys can be concluded according Figure 4. Although the amount of the second phase was increased little with the increase in Ca addition from 0 to 0.32%, the strength of the alloy was decreased due to the reduction of I-phase, which can significantly enhance the strength of the alloy. It has been reported that the elongation increased first and then decreased with the increasing of Ca content, and it was caused by the increasing content of  $Mg_2Ca$  which dispersed at the grain boundary and could be the crack source [16, 25, 26]. This phenomenon also can be found in present study, in which the 0.32% Ca-containing alloy exhibited the best elongation. When the Ca addition increased to 0.64%, the increasing amount of  $Mg_2Ca$  and other larger second phase which can cause stress concentration lead to the decrease of the elongation and increase of strength.

## 5. Conclusion

With the addition of Ca,  $Mg_2Ca$  and  $Mg_6Zn_3Ca_2$  appear in the alloy and the I-phase tends to transfer into W-phase. As a consequence, both strength and elongation of the as-cast alloys are somewhat decreased. The optimized concentration of Ca addition is about 0.32 wt.% for as-cast Mg-7.2Zn-2.4Gd alloy. After extrusion, the grain size is found to be refined obviously with the addition of Ca and the elongation is somewhat enhanced to 13.6% when the Ca addition is increased to 0.32%. The elongation begins to decrease sharply when the Ca addition is increased to 0.64% due to the increased amount of large second phases, which can cause stress concentration, resulting in fracture.

## Data Availability

The data used to support the findings of this study are included within the article. The data are available from the corresponding author upon request.

## Conflicts of Interest

The authors declare that they have no conflicts of interest.

## Acknowledgments

The authors acknowledge the financial supports from the Program for Innovation Teams in University of Chongqing (Grant no. CXTDX201601032).

## References

- [1] D. Shechtman, I. Blech, D. Gratias, and J. W. Cahn, "Metallic phase with long-range orientational order and no translational symmetry," *Physical Review Letters*, vol. 53, no. 20, pp. 1951–1953, 1984.
- [2] Z. Luo, S. Zhang, Y. Tang, and D. Zhao, "Quasicrystals in As-cast Mg-Zn-RE alloys," *Scripta Metallurgica et Materialia*, vol. 28, no. 12, pp. 1513–1518, 1993.
- [3] M. Yamasaki, K. Hashimoto, K. Hagihara, and Y. Kawamura, "Effect of multimodal microstructure evolution on mechanical properties of Mg-Zn-Y extruded alloy," *Acta Materialia*, vol. 59, no. 9, pp. 3646–3658, 2011.

- [4] M. Yamasaki, K. Hashimoto, K. Hagihara, and Y. Kawamura, "Multimodal microstructure evolution in wrought Mg-Zn-Y alloys with high strength and increased ductility," *Materials Science Forum*, vol. 654-656, pp. 615-618, 2010.
- [5] J. Y. Lee, D. H. Kim, H. K. Lim, and D. H. Kim, "Effects of Zn/Y ratio on microstructure and mechanical properties of Mg-Zn-Y alloys," *Materials Letters*, vol. 59, no. 29-30, pp. 3801-3805, 2005.
- [6] S. D. Wang, D. K. Xu, X. B. Chen, E. H. Han, and C. Dong, "Effect of heat treatment on the corrosion resistance and mechanical properties of an as-forged Mg-Zn-Y-Zr alloy," *Corrosion Science*, vol. 92, pp. 228-236, 2015.
- [7] H. Yan, R. Chen, N. Zheng, J. Luo, S. Kamado, and E. Han, "Effects of trace Gd concentration on texture and mechanical properties of hot-rolled Mg-2Zn-xGd sheets," *Journal of Magnesium and Alloys*, vol. 1, no. 1, pp. 23-30, 2013.
- [8] D. Wu, R. S. Chen, and E. H. Han, "Excellent room-temperature ductility and formability of rolled Mg-Gd-Zn alloy sheets," *Journal of Alloys and Compounds*, vol. 509, no. 6, pp. 2856-2863, 2011.
- [9] S. H. Park, B. S. You, R. K. Mishra, and A. K. Sachdev, "Effects of extrusion parameters on the microstructure and mechanical properties of Mg-Zn-(Mn)-Ce/Gd alloys," *Materials Science and Engineering: A*, vol. 598, pp. 396-406, 2014.
- [10] H. Huang, Y. Tian, G. Yuan, C. Chen, W. Ding, and Z. Wang, "Formation mechanism of quasicrystals at the nanoscale during hot compression of Mg alloys," *Scripta Materialia*, vol. 78-79, pp. 61-64, 2014.
- [11] H. Huang, C. Chen, Z. Wang, Y. Li, and G. Yuan, "Effect of pretreatment and annealing on microstructure and mechanical properties of Mg-1.5Zn-0.25Gd (at%) alloys reinforced with quasicrystal," *Materials Science and Engineering: A*, vol. 581, pp. 73-82, 2013.
- [12] Y. Liu, G. Y. Yuan, C. Lu, and W. J. Ding, "Stable icosahedral phase in Mg-Zn-Gd alloy," *Scripta Materialia*, vol. 55, no. 10, pp. 919-922, 2006.
- [13] D. K. Xu and E. H. Han, "Effects of icosahedral phase formation on the microstructure and mechanical improvement of Mg alloys: a review," *Progress in Natural Science: Materials International*, vol. 22, no. 5, pp. 364-385, 2012.
- [14] H. Huang, H. Kato, C. Chen, Z. Wang, and G. Yuan, "The effect of nanoquasicrystals on mechanical properties of as-extruded Mg-Zn-Gd alloy," *Materials Letters*, vol. 79, pp. 281-283, 2012.
- [15] G. Yuan, Y. Liu, W. Ding, and C. Lu, "Effects of extrusion on the microstructure and mechanical properties of Mg-Zn-Gd alloy reinforced with quasicrystalline particles," *Materials Science and Engineering: A*, vol. 474, no. 1-2, pp. 348-354, 2008.
- [16] E. Zhang and L. Yang, "Microstructure, mechanical properties and bio-corrosion properties of Mg-Zn-Mn-Ca alloy for biomedical application," *Materials Science and Engineering: A*, vol. 497, no. 1-2, pp. 111-118, 2008.
- [17] B. Zhang, Y. Wang, L. Geng, and C. Lu, "Effects of calcium on texture and mechanical properties of hot-extruded Mg-Zn-Ca alloys," *Materials Science and Engineering: A*, vol. 539, pp. 56-60, 2012.
- [18] Y. Z. Du, M. Y. Zheng, X. G. Qiao et al., "The effect of double extrusion on the microstructure and mechanical properties of Mg-Zn-Ca alloy," *Materials Science and Engineering: A*, vol. 583, pp. 69-77, 2013.
- [19] L. Geng, B. P. Zhang, A. B. Li, and C. C. Dong, "Microstructure and mechanical properties of Mg-4.0Zn-0.5Ca alloy," *Materials Letters*, vol. 63, no. 5, pp. 557-559, 2009.
- [20] Y. A. Chen, H. Liu, R. Ye, and G. Liu, "Effects of the addition of Ca and Sb on the microstructure and mechanical properties of AZ91 magnesium," *Materials Science and Engineering: A*, vol. 587, pp. 262-267, 2013.
- [21] M. Yang, L. Cheng, and F. Pan, "Comparison about effects of Ce, Sn and Gd additions on as-cast microstructure and mechanical properties of Mg-3.8Zn-2.2Ca (wt%) magnesium alloy," *Journal of Materials Science*, vol. 44, no. 17, pp. 4577-4586, 2009.
- [22] R. Sun, Z. Wang, N. Shibata, and Y. Ikuhara, "A dislocation core in titanium dioxide and its electronic structure," *RSC Advances*, vol. 5, no. 24, pp. 18506-18510, 2015.
- [23] Z. Wang, M. Saito, K. P. McKenna, and Y. Ikuhara, "Polymorphism of dislocation core structures at the atomic scale," *Nature Communications*, vol. 5, no. 1, p. 3239, 2014.
- [24] Y. Lü, Q. Wang, W. Ding, X. Zeng, and Y. Zhu, "Fracture behavior of AZ91 magnesium alloy," *Materials Letters*, vol. 44, no. 5, pp. 265-268, 2000.
- [25] Z. Wang, M. Saito, K. P. McKenna et al., "Atom-resolved imaging of ordered defect superstructures at individual grain boundaries," *Nature*, vol. 479, no. 7373, pp. 380-383, 2011.
- [26] R. Sun, Z. Wang, M. Saito, N. Shibata, and Y. Ikuhara, "Atomistic mechanisms of nonstoichiometry-induced twin boundary structural transformation in titanium dioxide," *Nature Communications*, vol. 6, no. 1, p. 7120, 2015.



**Hindawi**  
Submit your manuscripts at  
[www.hindawi.com](http://www.hindawi.com)

